Surface Measurement Using Scanning Electron Microscope

Taras Vynnyk
Institute of Measurement and Automatic Control, Leibniz Universität Hannover
Nienburger Str. 17, 30167 Hannover, Germany
email: taras.vynnyk@imr.uni-hannover.de

Abstract
An improved photometric method for recording a 3D-microtopogrpahy of technical surfaces will be presented. The suggested procedure employs a scanning electron microscope (SEM) as multi-detector system. The improvement in measurement is based on an extended model of the electron detection used to evaluate the detectors signals in a different way compared to known approaches. The photometrical method is discussed both for convex and arbitrary surfaces.

Keywords:
Scanning Electron Microscope (SEM), photometric method

1 INTRODUCTION

The micro-topography of technical surfaces plays an important role for the functional behaviour of many mechanical parts in machinery. In order to make a proper assumption about this functional behaviour, these surfaces need to be measured fast, sufficiently accurate and, if possible, in non contact mode. Due to the fact that the modern technical surfaces often have very small structures, the requested lateral/vertical resolution should lie within a range from 30 to 50 nm. In this case the measurement problem can not be solved using standard measuring optical methods, which lateral resolution is limited by the wavelengths of the visible spectrum to ca. 200nm. Because of special form of stylus tip, the tactile devices also cannot be applied for the measurement of arbitrary structures (especially small concave areas). The highest lateral and vertical resolutions are reached with atomic force microscopes (AFM). However due to the long measuring times and small vertical measuring range, which is limited to few micrometers, it is difficult to apply AFM for the measurement of the large structures.

2 PROJECT PURPOSE

The purpose of this project is the development of 3D reconstruction method from SE-images, recorded by the scanning electron microscope. The advantage of this approach lies in very high lateral resolution (approx. 10 nm) in comparison to the standard measuring methods and in the large working distance (10 to 30 mm). A further advantage is the possibility to measure steep flanks with an inclination angle up to 85°.

The functional principle of the scanning electron microscope is shown on the figure 1. The electrons are thermionically emitted from an electron gun. After acceleration in the electric field toward the anode, the emitted electrons become the energy up to 100 keV and are focused by condenser lenses. The focused electron beam passes through pairs of scanning coils or pairs of deflector plates, which deflect the beam in the x and y axes so that it scans line by line over a rectangular area of the specimen surface. The intensity of the primary electron beam has a narrow Gauss - form with a standard deviation about 5-10nm.

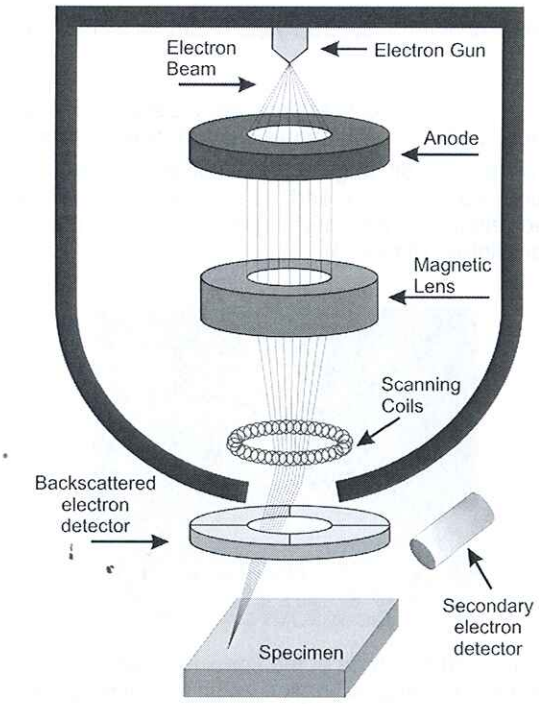

Figure 1: Functional principle of the scanning electron microscope, © IMR

With the penetration into the material the initiating electrons are slowed down due to multiple elastic and inelastic scatterings with the atoms of the material. According to the general agreement, all electrons with the energy within the range 0 and 50 eV are considered to be pure secondary electrons (SE1). The maximum withdrawal depth of the SE1 depends on the material and varies from 1 – 3 nm for metals to 10 – 20 nm for insulators [1]. The electrons with the energy more than 50 eV are called backscattered electrons (BSE). These electrons have a substantially larger emission volume that depends on the energy of the primary electron beam and can reach up to 200 nm. On the way from the material, the backscattered electrons produce further low-energy electrons (so called SE2, see figure 2).

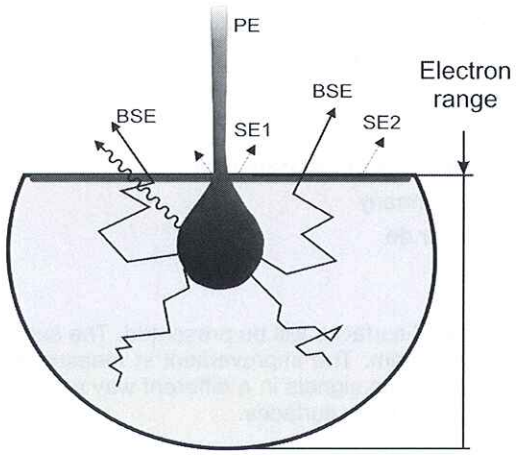

Figure 2: Emission of the electrons via elastic scattering, © IMR

The total secondary electron yield σ can be written as:

$$\sigma = \eta + \delta \quad (1)$$

where η means backscattered coefficient and δ is the emission coefficient of the pure secondary electrons.

With increasing tilt angle of the specimen the effective emission surface area and as a result the number of emitted electrons become larger. Therefore the flanks appear brighter (figure. 3).

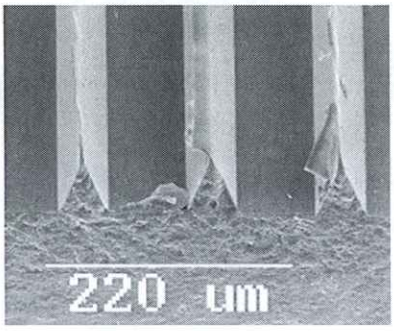

Figure 3: SEM Image of the specimen with the steep flanks. Due to steep inclination angle the flanks appear to be brighter as the horizontal areas, © IMR

In case of the surface irradiation with high-energy electrons the emission yield behaves like 1/cos of the inclination angle. With decreasing energy this growth becomes clearly weaker.

3 PROCEDURE

Despite its very high lateral resolution and the good signal to noise ratio on steep flanks, the scanning electron microscope has a huge disadvantage, namely it produces only to 2D images. In order to obtain the 3D topography some additional analysis steps are necessary. One distinguishes between the photogrammetric and the photometric 3D reconstruction methods.

3.1 Photogrammetric Method

This method is based on the evaluation of stereo images, which are generated by simple tilt of the specimen, as shown in the figure 4. The 3D- surface reconstruction does not require any modification of the scanning electron microscope and can by realized using proper software only. This method was developed in the 90's and is realized in the commercial software, e.g. MeX 3D by Alicona company. Since the electron emission yield depends on the inclination angle of the illuminated surface, the sample cannot be arbitrarily strongly tilted. Otherwise, the images would be so strongly distorted that the correspondence between individual points cannot be detected anymore. The maximal inclination angle, at which the images are still similar, is limited to 7 - 10°.

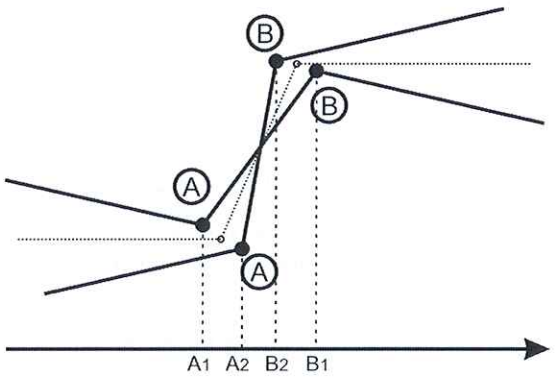

Figure 4: Schematic principle of the photogrammetric reconstruction, © IMR

A further disadvantage of the photogrammetric method is its inability to reconstruct the smooth surfaces. For the successful photogrammetric surface reconstruction it is necessary to find the correspondence between individual points in stereo images using correlation methods. The sensitivity of the correlation result depends very strongly on the correlating images. If the common overlap area contains some strong outliers in the form of structural components, then these are considered as orienting points. If the common overlap area is homogeneous, then the correlation result becomes almost constant and therefore vulnerable to noise.

One of the standard solutions is to spread reference objects, the so called nano-markers, on the surface of the specimen. Thus very high vertical resolution (up to 10 Nm) can be reached. This approach was developed at the company „M2C Microscopy Measurement & Calibration" and is used for the calibration of other methods on regular structures.

3.2 Photometric Method

The basics of the photometric method for the 3D-topography reconstruction from SEM images was developed already in the 80's - 90's by professor Reimer and his group at the University of Münster [1].

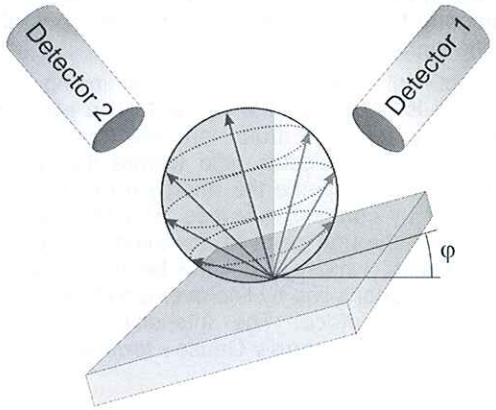

Figure 5: 2-detector system, © IMR

The procedure uses the Lambert's dependence of the angular distribution of the emitted electrons and $\cos^{-1}$ dependence of the emission yield from the inclination angle, see figure 5. For the detection of the emitted electrons 2 oppositely placed detectors are used [2]. The

employment of such setup leads to a higher efficiency by the registration of the SE.

Rekonstruction of convex areas

Firstly the simplest case, namely the electron emission from convex surfaces, would be examined. On the assumption that the efficiency of the detector system is 100%, all emitted electrons by detectors would be registered by one of the detectors. Such kind of emission can be replaced by emission from the tangential level:

$$z - z(x_0, y_0) - \frac{\partial z(x_0, y_0)}{\partial x}(x - x_0) - \frac{\partial z(x_0, y_0)}{\partial y}(y - y_0) = 0 \qquad (2)$$

Without loss of generality the origin of the global coordinate system (GCS) will be set to the currently examined point (x_0, y_0).

For registering the emitted electrons 2 detectors with the same collecting efficiency are used. The detectors are aligned along the Y-axis, so that all electrons with the initial velocity to the right of the XZ plane are registered by detector 1, while all initially left-oriented electrons are collected be detector 2. Since the emission yield is dependent of the local inclination of the surface, a new local coordinate system (LCS) is introduced, so that the emission plane will be considered as XY plane, and both detectors would be placed in the YZ – plane (figure 6).

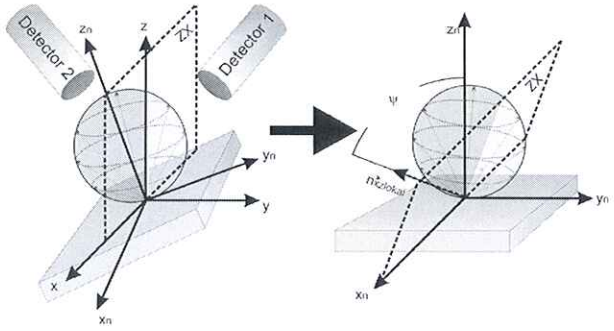

Figure 6: Emission in Global (left) and local (right) coordinate systems, © IMR

After the transition to the local coordinate system the detector signals are computed:

$$I_{1y} = k \cdot \sigma(x, y)\left(\tfrac{1}{2} - \sin\psi_y\right) \qquad (3)$$

With k – constant amplification factor of the detector, ψ_y – projection of the emission angle on the ZY plane.

Thus a conclusion about the functional dependence between the local gradient of the surface in Y- direction and the detector signals is possible:

$$k_y(x, y) = \frac{I_{2y} - I_{1y}}{I_{2y} + I_{1y}} = \frac{\frac{\partial z}{\partial y}}{\sqrt{1 + \frac{\partial z}{\partial y}^2 + \frac{\partial z}{\partial x}^2}} \qquad (4)$$

In case the detectors are aligned along the X axis, the equation (4) would be transformed into (5):

$$k_x(x, y) = \frac{I_{2x} - I_{1x}}{I_{2x} + I_{1x}} = \frac{\frac{\partial z}{\partial x}}{\sqrt{1 + \frac{\partial z}{\partial y}^2 + \frac{\partial z}{\partial x}^2}} \qquad (5)$$

Strictly speaking, for exact surface reconstruction it is necessary to have 4 detectors. 2 should be aligned along the X axis and 2 - along the Y axis. Another possibility is to use only 2 detectors and the rotation unit around Z axis. The solution of the equations set (4) - (5) supplies partial derivatives of the topography:

$$\frac{\partial z(x,y)}{\partial x} = \frac{k_x(x,y)}{\sqrt{1 - k_x(x,y)^2 - k_y(x,y)^2}}, \quad \frac{\partial z(x,y)}{\partial y} = \frac{k_y(x,y)}{\sqrt{1 - k_x(x,y)^2 - k_y(x,y)^2}} \qquad (6)$$

Finally the surface will be reconstructed using numeric integration.

Rekonstruction of arbitrary areas

Usually electrons with the small emission angle are reabsorbed from the specimen surface. As the result the efficiency of detectors becomes smaller than 100% and the solution (6) for the surface reconstruction is not valid anymore. Since the surface is a-priori unknown, the solution of the problem can be reached only by iterative correction of the previous reconstruction results.

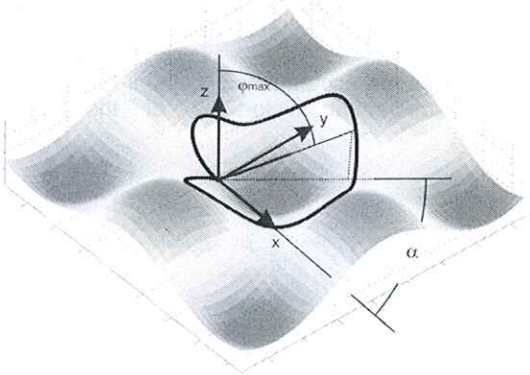

Figure 7: Evaluation of the non-detectable emission fraction, © IMR

In the figure 7 the arbitrary topography is presented. The primary electron beam irradiates the specimen in the point (0,0). In order to be registered by any detector, the emission electrons must have a steep exit angle. For each azimuthal angle α there exists minimal exit angle $\varphi_{min}(\alpha) = \pi/2 - \varphi_{max}(\alpha)$ (see figure 7), at which electrons touch the surface. These minimal angles could be calculated from the black drawn strip line in the figure 7.

The detector signal $I^*_{1y}(x, y)$ can be evaluated as follows:

$$I^*_{1y}(x, y) = I_{1y}(x, y) - k \cdot \sigma(x, y)\lambda_{1y}(x, y) \qquad (7)$$

where $\lambda_{1y}(x, y) = \frac{1}{\pi}\int_0^{\pi} \cos^2 \varphi_{\min}(\alpha) \cdot d\alpha$ describes the relative fraction of non-registered electrons by recording of the Signal $I^*_{1y}(x, y)$ and k – constant amplification. The function $I_{1y}(x, y)$ can be evaluated using Eq. (3). The non-registered fractions λ_{2y}, λ_{1x} and λ_{2x} for other detectors (second detector in the y-axis, and both detectors in the x-axis) should be calculated using the same principles.

Under the influence of the not registered fractions the expressions for the partial derivatives (6) will be changed [3]:

$$\frac{\partial z(x,y)}{\partial x} = \frac{\tilde{k}_x(x,y)}{\sqrt{1 - \tilde{k}_x(x,y)^2 - \tilde{k}_y(x,y)^2}}, \quad \frac{\partial z(x,y)}{\partial y} = \frac{k_y(x,y)}{\sqrt{1 - \tilde{k}_x(x,y)^2 - \tilde{k}_y(x,y)^2}} \qquad (8)$$

with

$$\tilde{k}_x(x, y) = k^*_x(x, y) \cdot (1 - \lambda_{2x} - \lambda_{1x}) - \lambda_{1x} + \lambda_{2x}$$
$$\tilde{k}_y(x, y) = k^*_y(x, y) \cdot (1 - \lambda_{2y} - \lambda_{1y}) - \lambda_{1y} + \lambda_{2y} \qquad (9)$$

Finally the reconstruction algorithm can be defined as follows:

1. With the 0-Iteration the surface is supposed to be convex and the partial derivatives will be computed according to eq. (3).
2. Numerical integration of the partial derivatives.
3. Evaluation of the not registered factions λ_{1y}, λ_{2y}, λ_{1x} and λ_{2x} basing on the reconstruction results from step 2.

4. Correction of the derivatives according eq. (8) - (9) and numerical integration.
Usually the computed surface converges very fast to the actual one (5 - 7 iteration steps).

3.3 Numeric integration and error analysis

As already mentioned, the surface is determined using numeric integration of the partial derivatives:

$$z(x^*, y^*) = \int_0^{x^*} \frac{\partial z(x,0)}{\partial x} dx + \int_0^{y^*} \frac{\partial z(x^*, y)}{\partial y} dy \qquad (10)$$

Beside the deterministic information every measuring system contains also stochastic noise. In the photometric method this stochastic fraction plays an important role, since the errors are accumulated by the integration, which leads to substantial distortions of the calculated topography.

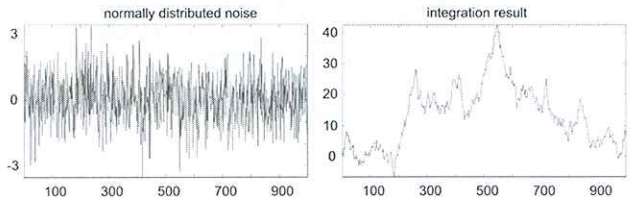

Figure 8: Noise integration, © IMR

The figure 8 clarifies this problem. Here the normally distributed noise (left) was integrated (right). The antiderivative possesses very big deviations (in the comparison to the noise) to the desired value, which should be equal to 0. Due to the assumption that the partial derivatives of the surface function are differentiable, the integration (eq. 10) can be performed along arbitrary smooth curves. In case the partial derivatives do not contain a stochastic fraction the integration results must be independent on the integration curves. The presence of the noise leads to different integration results. This fact offers the possibility to reduce the integration errors via averaging of the integration results over different curves. However the averaging will not be applied to the integration results directly. Firstly, the signals would be transformed in the frequency space using fast fourier transformation. Derivation in normal space is equal to the multiplication in the frequency area, see eq. 11.

$$\frac{\partial z(x,y)}{\partial x} \Leftrightarrow i\omega \cdot Z(\omega, \nu) \qquad (11)$$

where z(x, y): surface function
Z(ω, v): fourier transformation of the z(x, y)
ω, v: correspondent frequencies

So, while performing integration in the frequency space all noise components would smear over the whole integration area and thus „the cumulative error“ from noise would be radically reduced.

The algorithm was implemented in Matlab-Program and compared with the standard integration methods. The comparison results show, that the standard deviation as well as the form of the reconstructed surface using the “frequency” integration method are substantially improved.

4 SUMMARY

In this paper the photometric method for 3D surface reconstruction using SEM images was presented. The presented model was verified using the scanning electron microscope DSM940A with a 2-detector system. Since the 2-detector system is a custom made product, a control unit of the company Point Electronics was integrated. The experimental results show very good results, especially in flank area. Further improvement can be reached combining the photometric and photogrammetric methods.

5 ACKNOWLEDGEMENT

The work described in this paper is funded by the German Research Foundation (DFG) project “Riblets on Compressor Blades”.

6 REFERENCES

[1] Reimer, L.: Scanning Electron Microscopy, 2nd ed., Springer Series in Optical Science, Vol. 45, Berlin (1998)

[2] Lange, M., Reimer, L., Tollkamp, C.: Testing of Detector Strategies in Scanning Electron Microscopy, Journal of Microscopy Vol. 134/ 1984, pp. 1-12

[3] Vynnyk, T; Seewig, J., Reithmeier. E: 3D Oberflächenvermessung mit dem Niederspannungsrasterelektronenmikroskop, XII Internationales Oberflächenkolloquium Chemnitz 2008, Seite 102-109, ISBN 978-3-8322-6912-8